Evidence for the occurrence of a prototype structure in Sc under pressure

Y. C. Zhao,* F. Porsch, and W. B. Holzapfel
Fachbereich Physik, Universität-GH-Paderborn, D-33095 Paderborn, Germany
(Received 17 November 1995; revised manuscript received 11 April 1996)

Structures and pressure-volume relations of scandium under pressures up to 76 GPa have been studied at room temperature with diamond-anvil cells by energy-dispersive x-ray diffraction using synchrotron radiation. In contrast to previous studies, many more diffraction lines are recorded for Sc(II), stable from 17.2 to at least 76 GPa, the highest pressure of the present study. A pseudo-body-centered-cubic lattice with 24 atoms in the cubic cell results in a perfect indexing of all the diffraction lines observed and some information on the atomic arrangement is derived from the intensity pattern. Since no other element shows the same kind of diffraction pattern, this phase represents a new prototype structure, and Sc under pressure follows a special structural sequence with significant differences to the systematics observed in most of the other (trivalent) rare-earth metals. [S0163-1829(96)00738-2]

I. INTRODUCTION

Scandium with its one $3d$ electron in the outer shell of its free atoms represents the first member of the d-transition-metal group. Conventionally, Sc, Y and the lanthanide metals (L) are grouped together as the rare-earth (RE) metals[1] due to their similarities in their outer electron configurations and in many of their physical and chemical properties. However, in contrast to Sc, the trivalent L metals and Y undergo under pressure a common sequence of structural transitions in the direction[2–5] hcp($hP2$)→Sm-type($hR9$)→dhcp($hP4$)→fcc($cF4$)→distorted-fcc($hR24?$). Thereby the symbols in parentheses represent Pearson's notation, which is strongly recommended for more systematic use by International Union of Pure and Applied Chemistry (IUPAC).[6] At ambient pressure Sc crystallizes also in the $hP2$ structure and this phase is commonly denoted as Sc(I). The phase transition to Sc(II) was observed around 19 GPa first by superconductivity and by room-temperature resistance measurements,[7] and later confirmed by x-ray-diffraction measurements,[8,9] which indicated that Sc(II) does not belong to any of the regular RE structures, but might be characterized possibly by a primitive tetragonal lattice.[8,9] Moreover, by correlating the structural energies with the d-band occupancy, a first-principles calculation[10] resulted in the following structural sequence for Sc with increasing pressures: $hP2$-$cF4$-$hP3$(ω-phase)-$tP4$-$cI2$. Thereby the calculated atomic volumes at the $hP2$-$cF4$ and $cF4$-$hP3$ transitions were both close to the value observed experimentally for the Sc(I)→Sc(II) transition. Recently, a close resemblance in the phonon dispersion was observed in the high-temperature $cI2$ phases of Sc with respect to its neighboring group IVB metals, and therefore it was speculated[11] that the $hP2$-$hP3$ transition[12] found in the group IVB metals may also occur in Sc under pressure. However, according to the previous x-ray-diffraction studies[8,9] the structure of Sc(II) is distinctly different from the $hP3$ structure. Since the previous structural proposals were based only on measurements with conventional x-ray sources with contradictory interpretations of the poorly resolved patterns[8,9] and also in contrast with the theoretical predictions,[10] it appeared appropriate to use synchrotron radiation to obtain x-ray-diffraction patterns for Sc(II) with higher resolution to resolve its structure.

II. EXPERIMENTAL

The present experiments were performed with synchrotron radiation at HASYLAB, Hamburg, at the station for energy-dispersive x-ray-diffraction (EDXD) as described previously.[13,14] Pressures were generated with diamond-anvil cells[15,16] and inconel gaskets together with liquid nitrogen or mineral oil as pressure transmitting medium. Ruby powder served as a sensor for the pressure determination from the shift of the R_1 ruby luminescence line according to the nonlinear pressure scale.[17] Seven Sc samples were studied in order to test the reproducibility of the experimental results. Most of the experiments were performed with a diffraction angle 2θ around 10°, some others with $2\theta=5.644°$, corresponding to $Ed=12\,593.1$ keV pm, allowed us to recover also diffraction peaks with lattice spacings d_{hkl} up to 630 pm. The sample material was provided by K. A. Gschneidner, Jr., with chemical analysis indicating as major impurities in atomic ppm 294 for hydrogen, 306 for oxygen, 29 for iron, and 80 for lanthanides.

III. RESULTS AND DISCUSSION

$hP2$-Sc(I) is observed up to about 20 GPa in all the experiments but first signs of Sc(II) appear at 17.2 GPa, as shown in Fig. 1. Sc(II) remains stable at least up to 76 GPa, the highest pressure of the present study. Figure 2 shows EDXD spectra for Sc(II) at 31.0 GPa. The present diffraction spectra with their higher resolution show first of all that a large body-centered-cubic unit cell with $a=741.2(1)$ pm allows us to index all the observed peaks as shown in Fig. 3 and in Table I for a spectrum of Sc(II) taken at 31.0 GPa. This indexing was performed with the special software XPOWDER,[18] which searched for all possible structures within the cubic, tetragonal, orthorhombic, rhombohedral, and hexagonal systems, excluding only the monoclinic and triclinic systems due to their extremely large number of possibilities and very low likeliness for such a simple diffraction pattern,

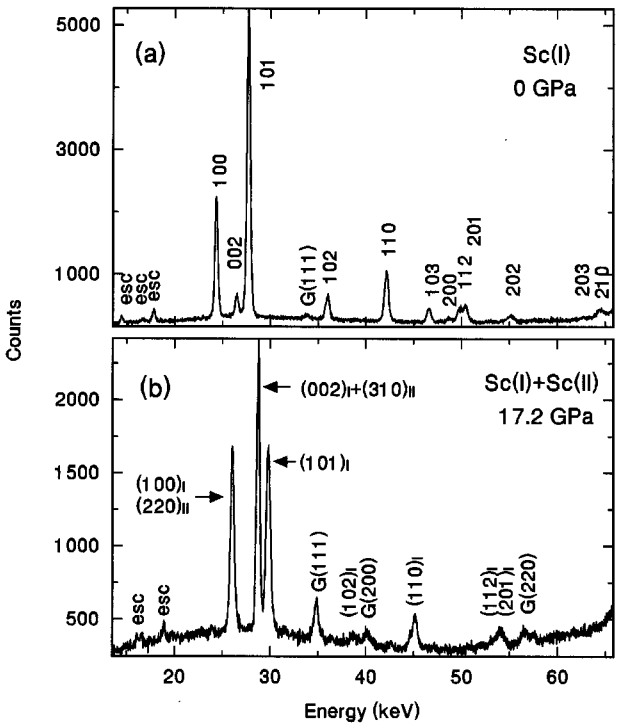

FIG. 1. EDXD spectra for $hP2$-Sc(I) at ambient pressure (a) and for the mixture of Sc(I) and Sc(II) at 17.2 GPa (b) taken with $Ed=6981.6$ keV pm corresponding to $2\theta=10.188°$. Escape peaks and diffraction peaks from the inconel gasket are denoted by esc and G, respectively.

allowing for unit-cell volumes up to 1 nm^3. This program resulted in only this solution or trivial equivalent indexing and all the observed lines are indexed by this scheme with a standard error of $\sigma=0.12\%$ with $\sigma=\{\Sigma[(d_{\rm obs}-d_{\rm cal})/d_{\rm obs}]^2/(N-1)\}^{1/2}$. This standard deviation fits to the typical experimental accuracy, and only three expected peaks in the experimental range down to 110 pm are not observed within the present sensitivity, recovering intensities down to 0.1% with respect to the largest intensity observed for the (310) peak. Only the peaks with intensities larger than 1.6% were observed in the previous studies[8,9] as shown in Fig. 3, where the present data are denoted by solid dots and previous data[9] by open circles. The previous proposals of different $tP4$ structures for the lattice of Sc(II) result in significantly larger values for σ ($>0.5\%$), and do not reproduce most of the weaker peaks discovered in the present measurements. Therefore, the previous assignments[8,9] with two different primitive tetragonal lattices can be ruled out whereas the present assignment of a bcc lattice for Sc(II) seems to result in a perfect fit.

Since the atomic volume for Sc(I) at the phase transition sets a lower limit to the number of atoms in the proposed unit cell for Sc(II), the most reasonable result is obtained for 24 atoms per unit cell, which leads to a volume decrease of 6.5% at the phase transition from Sc(I) to Sc(II), whereas 26 atoms in this unit cell would result in a rather large volume decrease of 13.7%. In Pearson's notation $cI24$ appears at this stage as the most likely structure and $cI26$ remains as an other possible candidate. Since none of the elements is known to crystallize in one of these structures at any

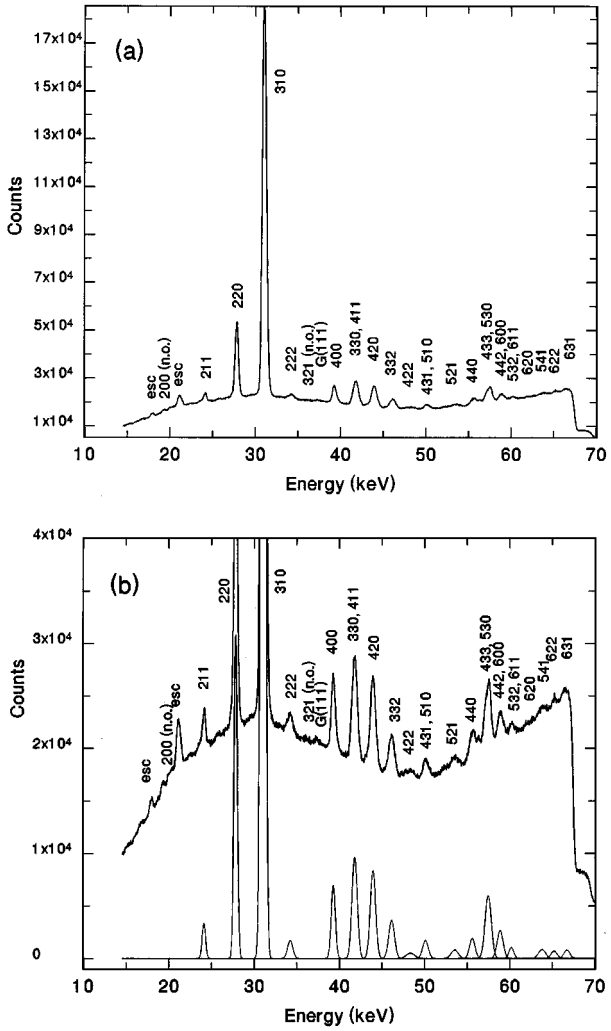

FIG. 2. EDXD spectrum for SC(II) at 31.0 GPa with $Ed=7289.1$ keV pm corresponding to $2\theta=9.575°$. The spectrum is indexed according to a bcc lattice with $a=741.2(1)$ pm. Escape peaks, diffraction peaks from the gasket, and the not observed peaks are denoted by esc, G, and n.o., respectively. The result of fitting Gaussian profiles to the observed diffraction peaks is shown in the lower part of (b).

condition,[4,19–23] Sc(II) presents a new prototype structure. In order to locate the atoms in this bcc unit cell, diffraction intensities were calculated and then compared with the observed diffraction intensities. There are nine space groups with a bcc lattice but only two of them, $I23$ and $I2_13$, need to be considered for these calculations, because all others are supergroups of these two. However, with full variation of the free atomic positional parameters for all possible combinations of site occupations for these two space groups, none of the calculated spectra agreed with the observed intensity data within the experimental uncertainty allowing also for some texture. This observation leads to a dilemma: an excellent agreement between observed and calculated d values and a poor agreement between observed and calculated intensities. To solve this dilemma one could assume that extremely strong but reproducible texture falsifies the observed intensity data or otherwise that the lattice of Sc(II) shows only some similarity to the proposed body-centered-cubic lattice

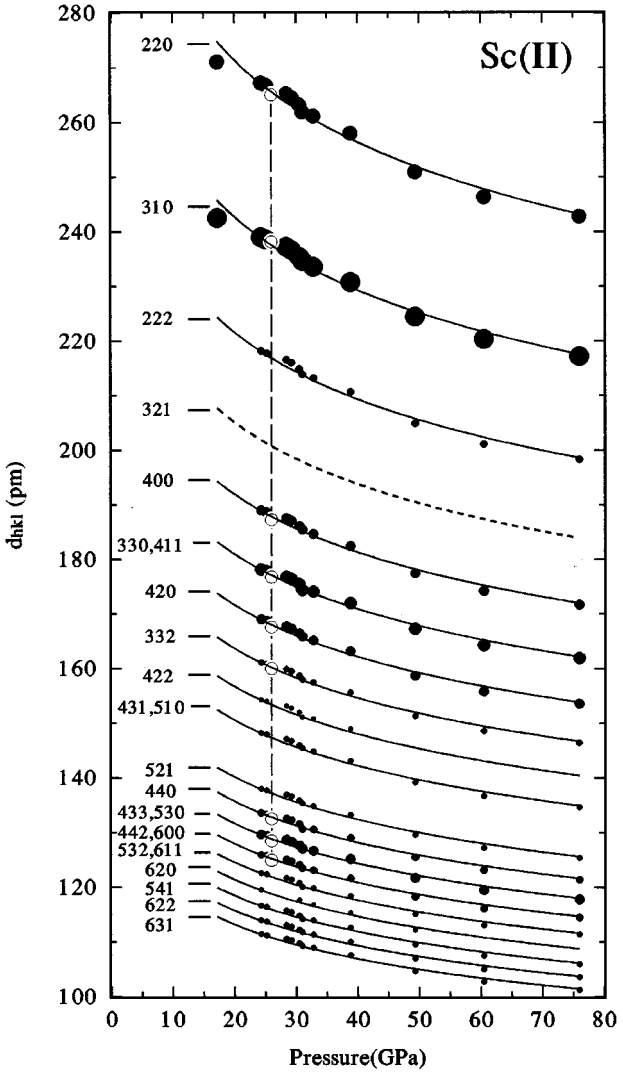

FIG. 3. d_{hkl} data for Sc(II) with the present indexing scheme. The present data are represented by solid circles with their sizes denoting the intensities of the corresponding diffraction peaks. The only set of data at 26.0 GPa given in Ref. 9 is represented by open circles.

but the actual symmetry of Sc(II) is lower than $I23$ or $I2_13$. The first case appears to be unlikely because all the present experiments show reasonably reproducible relative intensities which agree also qualitatively with the intensities observed in the earlier experiments.[8,9] Therefore, a pseudo-$cI24$ (or pseudo-$cI26$) structure fits best to the present data for Sc(II).

In order to make a more detailed structural proposal for Sc(II), one can start with the lowest symmetry space group $P1$ with the parameters of the triclinic unit cell $a=b=c=(\sqrt{3/2})a_{\rm bcc}$ and $\alpha=\beta=\gamma=109°28'$, where $a_{\rm bcc}$ is the unit-cell parameter of the bcc lattice, with the assignment of 12 or 13 atoms to the $1a$ position, and then determine 12×3 or 13×3 free parameters for the atomic positions. On the other hand, the structure of Sc(II) may be modeled by packing one structural unit in the lattice under the constraints of the combination of the point symmetry for the structural unit and the transitional symmetry for the lattice. For this

TABLE I. Measured intensities $I_{\rm obs}$ and lattice spacings $d_{\rm obs}$ for Sc(II) at 31.0 GPa in comparison with calculated values $d_{\rm cal}$ for a bcc unit cell with $a=741.2(1)$ pm. Miller indices hkl and the relative deviations $\Delta d/d$ of the fitted d values are also presented. M denotes the number of the $\{hkl\}$ faces with the same d spacing. n.o. denotes not observed peaks.

hkl	$I_{\rm obs}$	$d_{\rm obs}$ (pm)	$d_{\rm cal}$ (pm)	$(d_{\rm obs}-d_{\rm cal})/d_{\rm obs}$ (%)	M
110	n.o.	n.o.	524.1		12
200	n.o.	n.o.	370.6		6
211	1.7	302.1	302.6	−0.17	24
220	15.6	261.9	262.0	−0.04	12
310	100	234.7	234.4	0.13	24
222	1.4	213.9	214.0	−0.05	8
321	n.o.	n.o.	198.1		48
400	4.3	185.5	185.3	0.11	6
330,411	7.7	174.4	174.7	0.00	12,24
420	6.8	165.9	165.7	0.12	24
332	3.2	158.0	158.0	0.00	24
422	0.6	151.1	151.3	−0.13	36
431,510	1.5	145.5	145.4	0.07	48,24
521	0.9	135.4	135.5	0.07	48
440	1.6	130.7	131.0	−0.23	12
433,530	5.6	126.9	127.1	−0.16	24,24
442,600	2.4	123.7	123.5	0.16	24,6
532,611	0.8	120.1	120.2	−0.08	48,24
620[a]	<0.1	117.0	117.2	−0.17	24
541	0.6	114.2	114.4	−0.18	48
622	0.4	111.8	111.7	0.09	24
631	0.4	109.2	109.3	−0.09	48

[a]This peak has only marginal intensity.

approach, some special features of the spectra for Sc(II) should be noted: The (110) and (200) peaks have never been observed in any of the diffraction spectra with small diffraction angles, which extend into the appropriate range covering the d values of the (110) and (200) peaks: The absence of these two peaks cannot be attributed to texture because the corresponding higher-order reflections (220) and (400) are very well observed. The (321) peak with its large multiplicity factor has never been observed, and furthermore, the diffraction intensities seem to be modulated, suggestive of a specific cluster stacking in the structure of Sc(II). An icosahedral cluster, which consists of 12 atoms at the vertices and 1 atom at the center, is one of the most stable and densest packings, and possible spontaneous distortions of the cubo-octahedral atomic clusters of $cF4$ or $hP3$ into icosahedral clusters have been discussed before from the point of view of local energetics.[24] Stimulated by this approach, one may consider that the structure of Sc(II) could be built up by ideal or distorted icosahedral clusters. Since the diffraction intensities are proportional to the square of the total scattering factor $F_{\rm total}$, the present model would result in $F_{\rm total}=F_{\rm lattice}\times F_{\rm cluster}$, where $F_{\rm lattice}$ and $F_{\rm cluster}$ are the form factors for the bcc lattice and the atomic cluster, respectively. $F_{\rm lattice}=2$ for every (hkl) of the bcc lattice and $F_{\rm cluster}=\int\rho(r)\exp(ik\cdot r)d^3r$, where $\rho(r)$ is the electron density for the atomic cluster. Without any further knowledge, $\rho(r)$ can be expressed as a multipole expansion in spherical polar

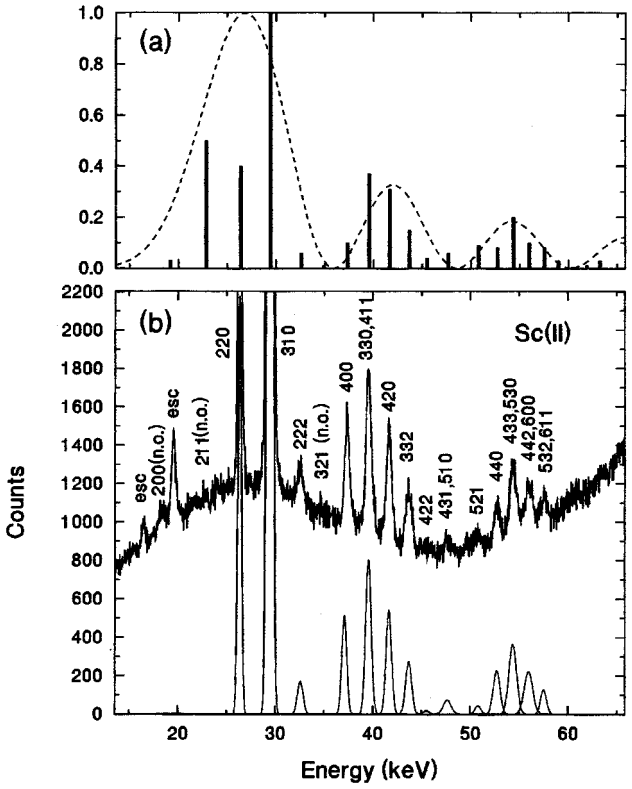

FIG. 4. Comparison of the model calculation for the intensities with an EDXD spectrum for Sc(II) at 29.2 GPa taken with $Ed = 6981$ keV pm corresponding to $2\theta = 10.188°$. The spectrum is indexed to a bcc lattice with $a = 748.5(2)$ pm. The variation of the relative intensities with respect to Fig. 2 indicates some effects of texture, most noticeable for (211). (a) illustrates by the dashed curve the variation of $[j_6(1.014ER\sin\theta)]^2$ for $R = 325$ pm together with calculated intensities by vertical solid bars according to the present model. The result of fitting Gaussian functions to the observed diffraction peaks is shown in the lower part of (b).

coordinates[25] and $\exp(ik\cdot r)$ can be expanded[25] in terms of spherical Bessel functions $j_l(kr)$ and harmonic functions $Y_{lm}(\theta,\phi)$. For the icosahedral cluster only the terms with $l=6$ dominate.[26] If the radial distribution of the electron density is approximated by a δ function with radius R corresponding to the size of the cluster, one arrives then at $F_{\text{cluster}} \propto j_6(kR)$. For the present EDXD method, the momentum transfer of photons scattered by the cluster is $k = 4\pi \sin\theta/\lambda = 1.014/(\text{pm keV})E \sin\theta$, where E is the photon energy. The values of $[j_6(kR)]^2$ with $R = 325$ pm are shown by the dashed line in Fig. 4(a), and Fig. 4(b) presents a diffraction pattern observed at 29.2 GPa for comparison. An atom located at $R=0$ would contribute to the term with $l=0$, however, having only the scattering power of $(1/13)^2$ with respect to the 12 remaining atoms of the cluster. For a real icosahedral cluster, F_{cluster} would depend also on the orientation of the clusters, represented by the values of $Y_{lm}(\theta,\phi)$. However, the integrated diffraction intensity results from all the lattice plans with the same d spacing averaged over all crystallites within the x-ray-irradiated region of the sample. The number of differently oriented planes with the same spacing is usually rather large as shown in Table I by the multiplicity M. Thus, if texture can be neglected, the orientation dependence of F_{cluster} may be averaged out largely and absorbed in the photon energy-independent prefactor in the formula for the calculation of integrated intensities.[27] The corresponding model calculations for such a simplified cluster scattering shows in Fig. 4 indeed some resemblance to the observed EDXD spectra for Sc(II), when the appropriate values for M, F_{lattice}, and F_{cluster} are used in the expression for the integrated intensities. The most obvious discrepancy between these calculated and observed intensities is then noticed for the (211) peak. This deviation could possibly be due to texture as indicated by the difference between the data illustrated in Figs. 1 and 2.

If one tries to work out a model of icosahedral-cluster packing, one finds that the detailed structure would depend on the orientation of the cluster with respect to the crystal axes. Without any knowledge of constraints upon the orientations of the cluster imposed by the site symmetries of the atoms, one can consider the constraints due to the cluster radius $R = 325$ pm related to the modulations in Fig. 4(a). Since $2R = 650$ pm corresponds to almost half of the body diagonal of the pseudo-bcc lattice $(\sqrt{3/2})a_{\text{bcc}} = 648$ pm at 29.2 GPa, the clusters would have to be linked by sharing common vertices along one of the body diagonals of the bcc unit cell. However, due to the symmetry of the icosahedron these arrays should not be linked by other common vertices. With this kind of linking, each pseudocubic lattice site would be occupied by 12 atoms, corresponding to a pseudo-$cI24$ structure for Sc(II). This pseudo-$cI24$ structural proposal or some similar quasicrystalline structure are furthermore supported by the observation that this structure would result for the volume decrease in the transition of Sc(I) to Sc(II) (as mentioned before) in a more reasonable value than the pseudo-$cI26$ structure, with its 13 atoms on each lattice site. Therefore, at this stage a pseudo-$cI24$ lattice is regarded as the most reasonable candidate for the structure of Sc(II).

With this structural model, the pressure dependence of the atomic volume can be calculated also for this phase to allow for a comparison with the data for Sc(I) and with some previous results for Sc(II),[28,29] as shown in Fig. 5. The present data for Sc(I) are consistent with the previous data, which can be represented by any of the common equation-of-state (EOS) forms using ambient pressure values for the atomic $V_0 = 0.02499$ nm^3, for the bulk modulus $K_0 = 60(1)$ GPa and for its pressure derivative $K_0' = 2.8(3)$. The small difference between the previous and the present data for the Sc(II) is partly caused by the different structural assignments, and the first data point in the transition region is considered to be less accurately determined due to phase mixture and the limited number of lines recorded in this case as shown in Fig. 3. Since the measured data cluster strongly around 30 GPa, five times stronger weight was given to the last two data at 60 and 76 GPa to obtain more reasonable results in the least-squares fitting of an analytic form to these data. Due to the small curvature in these data the common practice of using an EOS form with the three free parameters V_0, K_0, and K_0' for the volume, bulk modulus, and its pressure derivative extrapolated to zero pressure leads to large correlated uncertainties in these parameters for any of the common second-order EOS forms. This large ambiguity can be avoided to some extend, if one uses at first the convenient second-order form previously denoted[30] $H02$:

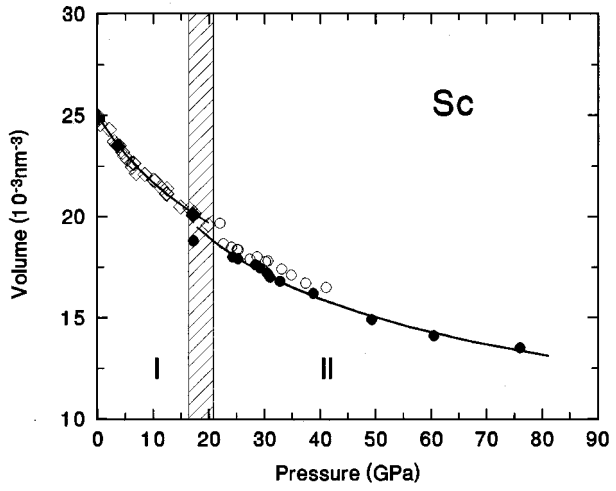

FIG. 5. Pressure-volume relation of Sc. Open symbols represent previous data (Refs. 29 and 30) and the solid symbols denote the present results with the assignment of the pseudocubic lattice $cI24$ to Sc(II). The solid curves represent fits using the EOS form $H02$ for Sc(I) and $H11$ for Sc(II) as discussed in the text. The mixed-phase region of Sc(I) and Sc(II) is denoted by the hatched area.

$p=3K_0(1-x)/x^5\exp[(3/2)(K_0'-3)]$ with $x=(V/V_0)^{1/3}$ and in a second step the closely related first-order form[31] $H11$, where $K_0'=3-\ln(3K_0/p_{\mathrm{FG0}})$ with the Fermi-gas pressure $p_{\mathrm{FG0}}=a_F(Z/V_0)^{5/3}$, the universal constant $a_{\mathrm{FG}}=0.02367$ GPa nm^5, and the total electron density Z/V_0 for ambient pressure guarantees the correct asymptotic variation at strong compression. In fact, many ''simple'' solids[31] follow this first-order form $H11$ over extremely wide ranges in pressure, and in the present case, the standard deviation of the fitted curve from the data even decreases slightly from $\sigma_v=0.653\%$ to 0.643% when this additional constraint is introduced for K_0', leading to $V_0=0.035(10)$ nm^3, $K_0=5.8(70)$ GPa, and the constrained value $K_0'=5.7$, whereby the standard deviations of the fitted parameters reflect only the statistical uncertainties. Thus one should note that these parameters serve only for the representation of the data, and the ability of the first-order form $H11$ to fit the EOS data may indicate, that these data represent a rather regular behavior typical for ''simple solids''[31] in contrast to the data for the low-pressure phase Sc(I) with their unusually small value for K_0', typical for the anomalous region of the ''regular'' RE metals, which is also characterized by unusually small values of K_0' due to s-d electron transfer.[4]

IV. CONCLUSION

The present EDXD data for Sc under pressures up to 75 GPa strongly support a different structural assignment for Sc(II) with respect to the previous results.[8,9] The present data for Sc(II) fit to a body-centered-cubic unit cell with 12 atoms clustered around each lattice point. The intensity data give some hints for possible icosahedral clusters or perhaps somewhat distorted icosahedra with typical size of $(\sqrt{3}/4)a_{\mathrm{bcc}}$ and with some kind of low-symmetry orientation in this structure breaking the cubic symmetry of the unit cell and leading therefore to a ''pseudo-$cI24$'' structural assignment. Since the observed diffraction patterns and the corresponding structural assignments are rather unique with no previous example of this structure type for any element under any condition, more detailed high-pressure x-ray-diffraction measurements using image plates with synchrotron radiation are desirable to provide some further information on this special structure. In addition, the range of the stability for this unusual structure should be explored also for later theoretical modeling.

ACKNOWLEDGMENTS

This work was supported in parts by the Bundesministerium für Forschung und Technologie (BMFT) under Grant No. 055PPAXB through DESY VI. The authors would like to thank Professor K. A. Gschneidner, Jr., for providing the sample material, W. Sievers for technical assistance, and J. Otto for support at the EDXD facility in HASYLAB. Y.C.Z. is indebted to the Alexander von Humboldt Foundation for financial support.

*Present address: Gordon McKay Laboratory, Division of Applied Sciences, Harvard University, Cambridge, MA 02138.

[1] K. A. Gschneidner, Jr., J. Alloys Compounds **192**, 1 (1993).
[2] A. Jayaraman and R. C. Sherwood, Phys. Rev. **134**, A691 (1964).
[3] D. B. McWhan and A. L. Stevens, Phys. Rev. **139**, A682 (1965).
[4] U. Benedict and W. B. Holzapfel, in *Handbook on the Physics and Chemistry of Rare Earths*, Vol. 17, edited by K. A. Gschneidner, Jr., L. Eyring, G. H. Lander, and G. R. Choppin (North-Holland, Amsterdam, 1993), p. 245.
[5] N. Hamaya, Y. Sakamoto, H. Fujihisa, Y. Fujii, K. T. Takemura, T. Kikegawa, and O. Shimomura, J. Phys. Condens. Matter **5**, L369 (1993).
[6] G. J. Leigh, *International Union of Pure and Applied Chemistry, Recommendations 1990* (Blackwell, Oxford, 1990).
[7] J. Wittig, C. Probst, F. A. Schmidt, and K. A. Gschneidner, Jr., Phys. Rev. Lett. **42**, 469 (1979).
[8] Y. K. Vohra, W. A. Grosshans, and W. B. Holzapfel, Phys. Rev. B **25**, 6019 (1982).
[9] J. Akella, J. Xu, and G. S. Smith, Physica **139&140B**, 285 (1986).
[10] P. Söderlind, Ph.D. thesis, Uppsala University, 1994.
[11] W. Petry, J. Trampenau, and C. Herzig, Phys. Rev. B **48**, 881 (1993).
[12] H. Xia, G. Parthasarathy, H. Luo, Y. K. Vohra, and A. L. Ruoff, Phys. Rev. B **42**, 6736 (1990).
[13] W. A. Grosshans, E.-F. Düsing, and W. B. Holzapfel, High Temp. High Pressure **16**, 539 (1984).
[14] J. Otto, in *HASYLAB Annual Reports* 1993 (DESY, Hamburg, 1994), p. 931.
[15] K. Syassen and W. B. Holzapfel, Europhys. Conf. Abstr. **1A**, 75 (1975).
[16] W. B. Holzapfel, in *High Pressure Chemistry*, edited by H. Kelm (Reidel, Boston, 1978), p. 177.
[17] H. K. Mao, P. M. Bell, J. W. Shaner, and D. J. Steinberg, J. Appl. Phys. **49**, 3276 (1978).
[18] F. Porsch (unpublished).

[19] D. A. Young, *Phase Diagrams of the Elements* (University of California Press, Berkeley, 1990).
[20] Y. C. Zhao, F. Porsch, and W. B. Holzapfel, Phys. Rev. B **49**, 815 (1994).
[21] M. Winzenick, V. Vijayakumar, and W. B. Holzapfel, Phys. Rev. B **50**, 12 381 (1994).
[22] W. B. Holzapfel, J. Alloys Compounds **223**, 170 (1995).
[23] W. B. Holzapfel, Rep. Prog. Phys. **59**, 39 (1996).
[24] M. Hoare, Ann. N. Y. Acad. Sci. **279**, 186 (1976).
[25] E. N. Maslen, A. G. Fox, and M. A. O'Keefe, in *International Tables for Crystallography*, edited by A. J. C. Wilson (Kluwer, Dordrecht, 1992), Vol. C, p. 476.
[26] G. Venkataraman, D. Sahoo, and V. Balakrishnan, *Beyond the Crystalline State* (Springer-Verlag, Berlin, 1989).
[27] B. Buras and L. Gerward, Prog. Cryst. Growth Charact. **18**, 93 (1989).
[28] W. A. Grosshans, Ph.D. thesis, University of Paderborn, 1987.
[29] W. A. Grosshans and W. B. Holzapfel, Phys. Rev. B **45**, 5171 (1992).
[30] W. B. Holzapfel, in *Molecular Systems under High Pressures*, edited by R. Pucci and G. Piccitto (North-Holland, Amsterdam, 1991).
[31] W. B. Holzapfel, Europhys. Lett. **16**, 67 (1991).